Multi-Network TDOA: An opportunity for vessels radiolocation

Conference Paper · May 2017

DOI: 10.1109/EURONAV.2017.7954215

Ciro Gioia
European Commission

Michele Vespe
European Commission

Multi-Network TDOA: an opportunity for vessels radiolocation

Ciro Gioia, Francesco Sermi, Dario Tarchi, Michele Vespe, Vladimir Kyovtorov

E[1]European Commission, Joint Research Centre (JRC),
Directorate for Space, Security and Migration,
Demography, Migration & Governance Unit, Via E. Fermi 2749, I-21027 Ispra (VA), Italy
Email: {ciro.gioia, francesco.sermi,dario.tarchi, michele.vespe, and vladimir.kyovtorov}@jrc.ec.europa.eu

***Abstract*—Detection and localization of vessels can be carried out by exploiting the radiolocation approach. Nevertheless, the employment of radiolocalization far from the shore can be limited by the lack of enough receivers to perform a correct multi-lateration of the RF source. In order to solve this gap, mobile assets or base stations from different networks need to be exploited. In particular, within a given search area, a ship could deploy low-cost receivers on drifting buoys, balloons or RPAs, creating a network with several nodes.**

Although this opportunity allows to enhance the geometry of the system, it also introduces synchronization issues. Such issues are mainly related to the dissimilarities in hardware and/or software of the employed devices. A *"Multi-Network TDOA"* algorithm is proposed, in order to solve this problem. The developed approach allows to account for the different offsets among the included nodes. The algorithm is compared with the classic TDOA method using simulated data in different scenarios.

From the results it emerges that whereas the classical algorithm is strongly affected by the offset, the proposed approach is robust with respect to this parameter. Moreover, the maximum synchronism offset between the base network and the additional devices is evaluated. Finally, the optimization of the overall network, in terms of minimum number of additional receivers, is assessed.

***Keywords*—Radiolocalization, Multi-Network TDOA, Synchronization**

I. INTRODUCTION

The maritime domain is the everyday theater of a long list of illegal activities, which includes: trafficking of human beings, smuggling of any sort of goods, spilling of polluting substances, waste disposal, violations of protected areas, illegal fishing, and much more. Therefore, a reliable dynamic maritime picture is an indispensable tool for the competent authorities to detect the actors of these illegal activities, which may be perpetrated within a large area, often too wide to be constantly monitored.

Nowadays, a fundamental role in the enhancement of the Maritime Situational Awareness (MSA) is played by the Automatic Identification System (AIS) [1], which allows exploiting the information shared by the majority of vessels to constantly update the maritime picture. Because of its cooperative nature, the AIS cannot be considered an exhaustive source of information for the realization of an omni-comprehensive dynamic maritime picture. In this scenario, a potential tool to improve the MSA is represented by radiolocation of Radio Frequency (RF) emitters [2] [3]. Basically, radiolocation techniques allow the localization of a target by detecting and ranging the radio frequency signals that it emits for any kind of purposes [4]. Any RF signal, e.g. Global System for Mobile Communications (GSM), AIS, Digital Video Broadcasting (DVB), can be exploited for radiolocation and, more generally, any sort of radio signal. The main requirement of RF radiolocation, in order to be exploited in the maritime domain, is the availability of at least three not-aligned RF receivers operating in the same band, typically referred to as *"base station"*, within the range of the target-transmitter [5].

AIS receivers exploit the preamble of the message in order to extract timing information, but, since there is no regulation about the specific synchronization technique to be employed, each AIS manufacturer makes use of different points of the preamble to achieve this goal. Evidently this fact does not represent a problem *per se* when the objective is the decodification of the AIS message. Nevertheless, this aspect becomes fundamental whenever AIS signals are exploited for radiolocation purposes [6]. If devices of the same manufacturer are employed, the offset between the receivers (due to the different timing extraction implementation) is negligible, whereas if different receivers are used, the offsets could prevent the correct outcome of the radiolocation technique.

In order to fill in this gap, a *"Multi-Network TDOA (MN)"* algorithm has been designed. The concept is similar to the ones used to estimate the user position with a multi-constellation Global Navigation Satellite System (GNSS) receiver [7]. In particular, the proposed approach extends the traditional Time Difference Of Arrival (TDOA) technique, to exploit moving asynchronous base-stations by working out any synchronization problem. Hereby, the MN approach is introduced, described and validated in various simulated scenarios, demonstrating how it systematically overcomes the traditional TDOA approach in terms of localization capabilities. A typical scenario for the application of the proposed RF radiolocation technique is sketched in Fig. 1, where different networks are used together. $\widehat{t_i}$ is the timing error related to the different networks. From the figure, it emerges the opportunity to merge measurements from heterogeneous coast devices together with mobile assets. From the results, the benefits of the inclusion of heterogeneous moving base stations, either non-synchronized or with different accuracies, are evident: this approach may significantly increase the precision in retrieving the target's position. Moreover, the maximum tolerable asynchronism between the receivers included in the network has been estimated. The paper is structured as follows: Section II describes the

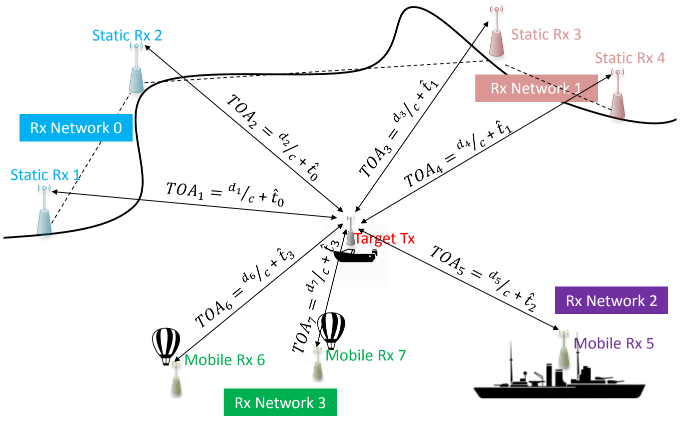

Fig. 1. Simplified scenario for the employment of RF radiolocation through *"MN"* algorithm.

MN algorithm, starting from the traditional TDOA approach; in Section III, the MN is validated with simulated data for different scenarios; finally, Section IV resumes the main achievements and presents some considerations.

II. Radiolocation Algorithms

The proposed algorithm has been developed to compute transmitter position using TDOA, as an extension of the classical TDOA technique. Hence, at first, the classical TDOA algorithm is presented in Section II-A, then its extension is discussed Section II-B.
The diagram of the algorithm is provided in Fig. 2, while the mathematical details and the description of the different blocks are discussed in the following sections.

A. Classical TDOA algorithm

TDOA classical algorithm relies on TDOA measurements obtained from Time Of Arrival (TOA) estimation [8], [9]. TOAs measurements are defined as [10]:

$$TOA = \frac{d}{c} + \widehat{t} + \epsilon_{TOA} = \frac{d}{c} + t_0^t + t_0^r + \epsilon_{TOA} \tag{1}$$

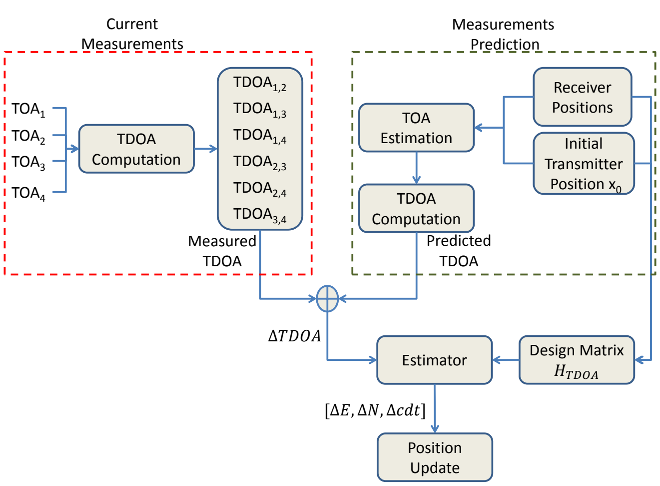

Fig. 2. Diagram of the TDOA localization algorithm.

where, t_0^t is the transmitter timing error, t_0^r is the receiver timing error, ϵ_{TOA} represents the residual error of the TOA measurement, c is the speed of light and d is the emitter-receiver distance, which expression is:

$$d = \sqrt{(E_T - E_R)^2 + (N_T - N_R)^2}, \tag{2}$$

where:

- E_T and N_T are the unknown coordinates of the emitter, expressed in the East North Up (ENU) frame;
- E_R and N_R are the receiver's coordinates, expressed in the ENU frame.

Eq. (1) cannot be directly used for the radiolocalization, because t_0^t is generally unknown and neglecting it can lead to large ranging uncertainties. Moreover, the transmitter timing error is device dependent and so generally unknown, because of differences in the electronics of dissimilar transmission equipment [11]. The simplest idea, in this case, is to compare the received TOAs pairwise and to use the TDOAs.

$$TDOA = TOA_i - TOA_j, \tag{3}$$

where TOA_i and TOA_j are the TOAs estimated respectively by the i^{th} and j^{th} receivers. By replacing Eq. (1) in the previous expression, one obtains:

$$TDOA_{i,j} = \frac{d_i}{c} + t_0^{r_i} + \epsilon_{TOA} - (\frac{d_j}{c} + t_0^{r_j} + \epsilon_{TOA}). \tag{4}$$

Neglecting the difference between the receiver's timing errors [12], $t_0^{r_i} - t_0^{r_j}$, leads to:

$$TDOA_{i,j} = \frac{d_i}{c} - \frac{d_j}{c} + \epsilon_{TDOA}. \tag{5}$$

TDOA measurements can be used for the localization using the approach shown in [13]. In particular, TDOA observables are not linear in the unknowns, hence a linearization process needs to be performed [14].
In order to linearize Eq. (5), it has to be expanded in Taylor series about the nominal position $\mathbf{x}_0 = [E_0, N_0]$. Truncating the expansion at the first order one obtains:

$$\begin{aligned} TDOA = TDOA_0 + \frac{\partial TDOA}{\partial E}|_{\mathbf{x}_0}(E - E_0) + \\ \frac{\partial TDOA}{\partial N}|_{\mathbf{x}_0}(N - N_0), \end{aligned} \tag{6}$$

where:

- $TDOA_0$ is the predicted TDOA, i.e. the TDOA evaluated in the approximate point x_0;
- $\frac{\partial TDOA}{\partial u}|_{\mathbf{x}_0}$ is the the partial derivative of the TDOA with respect to $\mathbf{u}$, evaluated in the approximate point, $\mathbf{x}_0$.

After some manipulation, Eq. (6) can be written as:

$$\delta TDOA = a\Delta E + b\Delta N, \tag{7}$$

where:

- $a = \frac{E_0 - E_R^1}{d_0^1} + \frac{E_0 - E_R^2}{d_0^2}$, $b = \frac{N_0 - N_R^1}{d_0^1} + \frac{N_0 - N_R^2}{d_0^2}$;
- $\delta TDOA = (TDOA - TDOA_0)$ is the difference between measured and predicted TDOA;

- ΔE and ΔN are respectively the East and North errors to correct the *a priori* position $\mathbf{x}_0$.

Since there are k TDOA measurements, a system of k Eq. (7) can be written in matrix notation:

$$\delta\mathbf{TDOA} = \begin{bmatrix} \delta TDOA_1 \\ \delta TDOA_2 \\ \vdots \\ \delta TDOA_k \end{bmatrix} = \begin{bmatrix} a_1 & b_1 \\ a_2 & b_2 \\ \vdots & \vdots \\ a_k & b_k \end{bmatrix} \begin{bmatrix} \Delta E \\ \Delta N \end{bmatrix} + \epsilon_{TDOA} \tag{8}$$

obtaining the compact expression:

$$\delta\mathbf{TDOA} = H_{TDOA}\Delta\mathbf{x} + \epsilon_{TDOA}, \tag{9}$$

where:

- $\Delta\mathbf{x}$ is the vector containing the unknowns $(\Delta E, \Delta N)$, which has to be evaluated using an estimation technique such as the Least Squares (LS) method;
- H_{TDOA} is the geometry matrix, which projects the measurements into the space domain;
- ϵ_{TDOA} is the vector containing the residual errors.

Finally, the user's coordinates can be computed as:

$$\mathbf{x} = \mathbf{x}_0 + \Delta\mathbf{x} \tag{10}$$

B. Multi-Network TDOA algorithm

The main limitation of the algorithm described in the previous section is the fact that the difference among the timing receiver errors is unknown. In fact, such a difference can lead to the divergence of the localization algorithm. When using nodes (receivers) with similar characteristics, belonging to the same network, $t_0^{r_i} - t_0^{r_j}$ can be calibrated or estimated with *a priori* information. If nodes with different characteristics are used, then $t_0^{r_i} - t_0^{r_j}$ cannot be calibrated or known *a priori*, hence another measurements model has to be adopted. In particular the TDOAs from dissimilar nodes (that is receivers with different characteristics) can be modeled as:

$$TDOA_{i,j} = \frac{d_i}{c} - \frac{d_j}{c} + c \cdot dt + \epsilon_{TDOA}, \tag{11}$$

where $c \cdot dt$ is the offset between the different clock of the nodes.
Eq. 11 is not linear in the unknowns, hence a linearization process has to be performed. In order to linearize Eq. (11), it has to be expanded in Taylor series about the approximate position $\mathbf{x}_{0,MN} = [E_0, N_0, cdt_0]$. Truncating the expansion at the first order one obtains:

$$\begin{aligned} TDOA = TDOA_0 + \frac{\partial TDOA}{\partial E}|_{\mathbf{x}_{0,MN}}(E - E_0) + \\ + \frac{\partial TDOA}{\partial N}|_{\mathbf{x}_{0,MN}}(N - N_0) + \frac{\partial TDOA}{\partial cdt}|_{\mathbf{x}_{0,MN}}(cdt - cdt_0). \end{aligned} \tag{12}$$

After the same manipulations carried out in the previous section, Eq. (12) can be written as:

$$\delta TDOA = a\Delta E + b\Delta N + f\Delta cdt, \tag{13}$$

where a and b have the same expression defined in the previous section and f assumes value one if the TDOA is between nodes with different characteristics and zero otherwise. In matrix notation Eq. (13) can be expressed as:

$$\delta\mathbf{TDOA} = \begin{bmatrix} \delta TDOA_1 \\ \delta TDOA_2 \\ \vdots \\ \delta TDOA_k \end{bmatrix} = \begin{bmatrix} a_1 & b_1 & 0 \\ a_2 & b_2 & 0 \\ \vdots & \vdots & \vdots \\ a_k & b_k & 1 \end{bmatrix} \begin{bmatrix} \Delta E \\ \Delta N \\ \Delta cdt \end{bmatrix} + \epsilon_{TDOA} \tag{14}$$

Although the algorithm has been described for the two dimensional case, implicitly assuming that maritime targets and receivers have all the same elevation (that is the sea level), it can be easily extended to the three dimensional case.

C. Geometrical Aspects

Positioning errors depend on the measurement accuracy and on the geometry of the receivers. Considering an *a priori* measurement accuracy σ_0 and assuming all the measurements uncorrelated and with the same accuracy, the state vector variance/covariance matrix can be expressed as:

$$DOP_{matrix} = \sigma_0^2 (H^T H)^{-1} \tag{15}$$

The matrix $(H^T H)^{-1}$ is related only to the receivers position, hence it represents the geometry of the system. Since the value of such parameter is generally greater than one, the accuracy is *diluted* so the matrix is usually referred to as Dilution Of Precision (DOP) matrix. Hence, positioning accuracy depends on different factors, such as: measurements errors, intrinsic quality of the signal measurement and geometry of the system. The latter is quantified by the DOP.
A measure of the overall quality of the LS solution, σ_{sol}, can be obtained by taking the square root of the sum of the parameter estimate variances:

$$\sigma_{sol} = \sqrt{\sigma_0^2 \sum_{k=1}^{P} DOP_{k,k}^2} \tag{16}$$

where P indicates the dimension of the DOP matrix. Hence each element of the state vector has a corresponding DOP value. The algorithms are developed in the ENU frame and the meaningful DOP parameters are listed below:

$$\begin{cases} EDOP = \sqrt{\sigma_0^2 DOP_{1,1}^2} \\ NDOP = \sqrt{\sigma_0^2 DOP_{2,2}^2} \\ PDOP = trace(DOP_{matrix}) \end{cases} \tag{17}$$

where East DOP (EDOP), North DOP (NDOP) and Position DOP (PDOP) are the DOP values relative to the East, North and Position components, respectively.

III. Validation Results

In this section, the experimental results obtained with the proposed algorithm are compared with that obtained using a classic TDOA localization algorithm.
In order to validate the robustness of the proposed approach, simulated data for different scenarios have been used. The setup adopted for the test is illustrated in Section III-A, whereas the results are discussed in Section III-B.

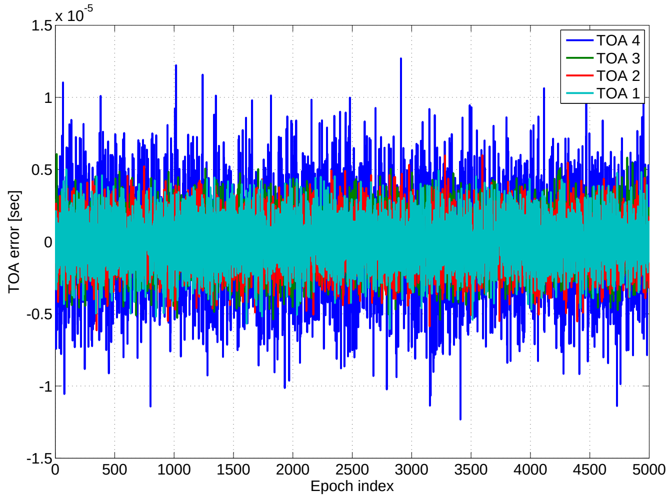

Fig. 3. TOA error plotted as a function of the time. The higher noise of the receiver number four (blue line) is evident.

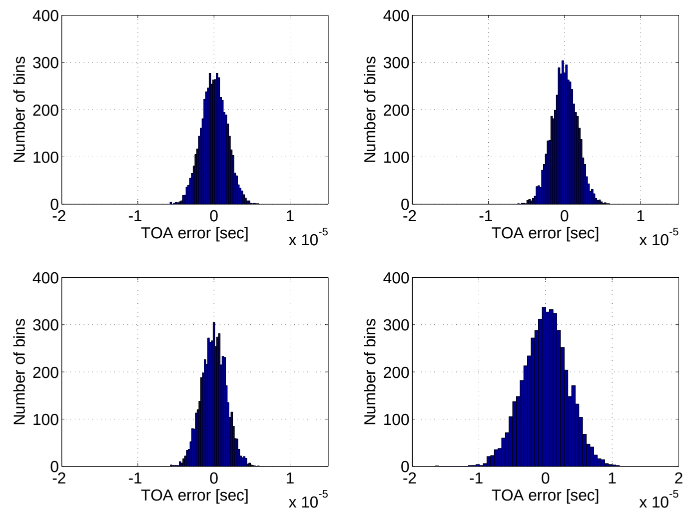

Fig. 4. TOA error distributions for the four receivers of the Base-line scenario.

A. Experimental Setup

In this section, the experimental setup adopted is described. To demonstrate the effectiveness of the algorithm described in Section II, three different scenarios have been simulated:

- **Base-line** $(3+1)$, where three receivers belonging to the same network and with the same characteristics are considered, along with one additional receiver with different characteristics. This scenario is exploited to analyze the relationship between the position errors and the time offset among different receivers.
- **Augmented** $(3+50)$, where three receivers belonging to the same network and with the same characteristic are considered, along with a variable number of receivers (between one and 50) with analogous performance. This scenario is used to evaluate the relationship between the position errors and the number of additional receivers.
- **Augmented** $(3+50)$ **degraded**, where three receivers belonging to the same network and with the same characteristics are considered, along with a variable number of receivers (between one and 50) with different characteristics. In this case the additional receivers are low cost, with reduced performance. This scenario is adopted to assess the impact of the introduction of low-cost receivers.

The simulated errors of the TOA measurement, considering three accurate receivers and one low cost receiver are shown in Fig. 3, where the TOA error is plotted as a function of the time. From the figure, it clearly emerges the higher noise of the receiver number four (blue line). TOA errors have been modeled as Gaussian processes with the following parameters: standard deviation equal to 500 m for high-end receivers and 1 km for low-cost receivers; mean equal to 10 m for high-end receivers and 20 m for low-cost receivers. The TOA error distributions of the four receivers are shown in Fig. 4. Evidently, the receiver number four is less accurate than the others: the relative bell is clearly larger than the others, which show similar distributions.

The developed algorithm exploits TDOA measurements, computed as detailed in Eq. (3). In the case of four receivers, six TDOAs are available: $TDOA_{1,2}$, $TDOA_{1,3}$, $TDOA_{1,4}$, $TDOA_{2,3}$, $TDOA_{2,4}$, $TDOA_{3,4}$. Since the fourth receiver has reduced performance, the measurements involving such receiver will present larger errors.

B. Experimental Results

This section presents the experimental results: in Section III-B1 those related to the base-line configuration, while in Section III-B2 those obtained using the augmented configurations.

1) Base-line configuration: The positions of receivers and target are shown in Fig. 5 in ENU coordinates, with the frame centered in a generic position, and defined as described in Section II.

In Fig. 6, the East, North and horizontal position errors are plotted as a function of time. The benefits of the adoption of the proposed algorithm are evident in the figure, where the

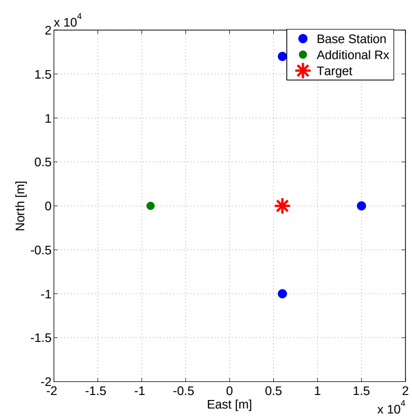

Fig. 5. Positions of receivers and target for the Base-line configuration. The positions are plotted in ENU coordinates, with frame centered in a generic position.

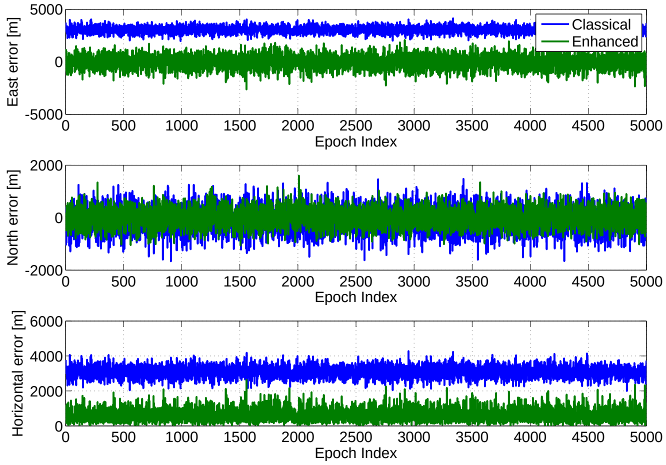

Fig. 6. East, North and Position errors as a function of the time. The benefits from the adoption of the proposed algorithm are evident: the main improvements are in the estimation of the East components. Moreover the computed error for the MN algorithm is always smaller than that of the classic algorithm, as it clearly appears for the East and the Horizontal position dimensions.

absolute position errors for the MN and the classical TDOA algorithms are compared along the three dimensions. To evaluate the effect of the offset between different receivers, a test using a different offset has been carried out. The performance of the classical and of the MN algorithms are evaluated in terms of Root Mean Square (RMS) and maximum position errors. The

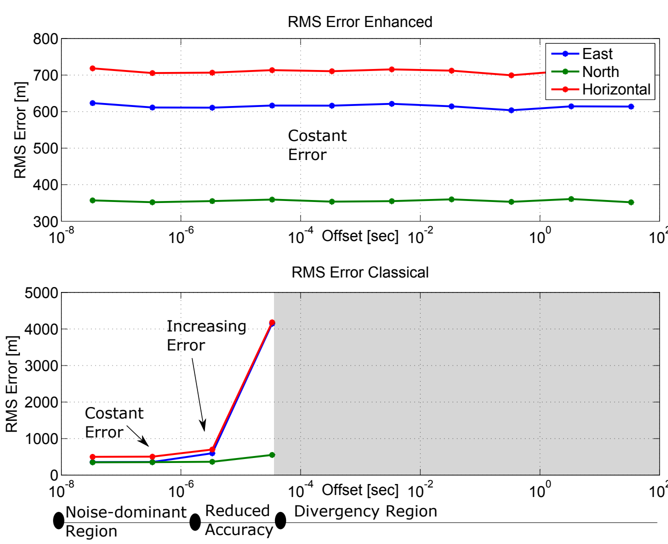

Fig. 7. RMS error for East, North and horizontal position dimensions as a function of the receiver offset. In the upper box the results obtained using he proposed method are illustrated whereas the results obtained with the classical algorithm are shown in the lower box.

results relative to the RMS of the East, North and Position error are shown in Fig. 7. In the upper box, the results obtained using the proposed method are illustrated, whereas the ones obtained with the classical algorithm are shown in the lower box. From the figure, it can be noted that the proposed algorithm is not affected by increasing the offset between the receivers. Contrarily, the classical algorithm is strongly affected by this parameter. In the first part, the classical algorithm seems to

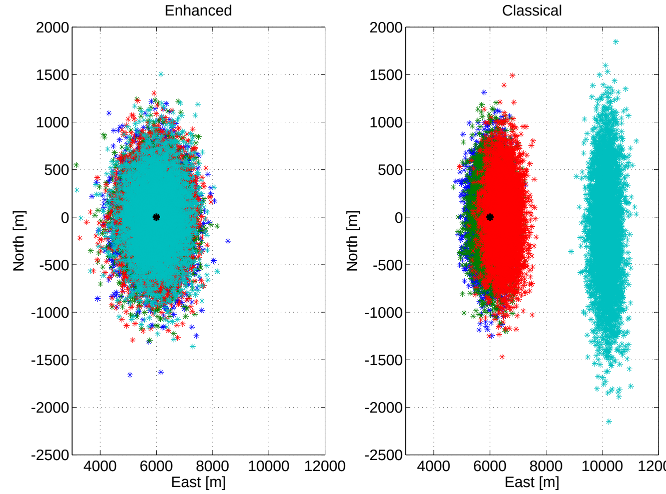

Fig. 8. Position of the target estimated with the classic (right) and with the MN (left) TDOA approaches. Each cloud is the result of 5000 processed samples and it is relative to a different value of the offset.

be robust to the variation of the offset, because the offset is absorbed by the stronger measurements noise; yet, when the offset becomes higher than the measurements noise the degradation is evident. With an offset longer than $3.3 \cdot 10^{-5}$ sec the algorithm does not converge anymore.

Finally, the estimated positions of the target are shown in Fig. 8: in the left box, the results of the proposed algorithm are shown, whereas in the right box, the results obtained using the classical algorithm are presented. Each cloud is relative to a different value of the receiver's offset, according to the four points in the lower box of Fig. 7. Comparing the two boxes of Fig. 8, it can be noted that all the clouds obtained using the MN algorithm are centered into the actual target position and are almost superimposed, while the clouds obtained with the classical algorithm clearly show the effect of the offset. In the right hand figure, a shift of the clouds to the right is evident and the cyan cloud appears spreading vertically more than the others.

2) Augmented configuration: In this section, the results obtained using the augmented configurations are presented. Specifically, two configurations are analyzed: one where an identical receiver is added to the network at each step; the other where one receiver with reduced performance is introduced at each step. The positioning of the additional receivers is random.

In Fig. 9, the displacement of the receivers is shown. The positions are plotted in the ENU local frame. The introduction of additional receivers improve the geometry conditions; in order to assess this improvement, the values of the EDOP, NDOP and PDOP as a function of the number of additional receivers are shown in Fig. 10. From the figure, two areas can be identified: the first region, where there is a high reduction of the geometric parameters; the second region (marked in grey in Fig. 10), where only a small improvement of the geometry can be appreciated. Hence, even though theoretically an infinite number of additional receivers can improve the geometric conditions, 20 additional devices seems to be a reasonable limit to achieve an appreciable improvement. Obviously, the geometry and the geometric improvements presented respectively in Fig.

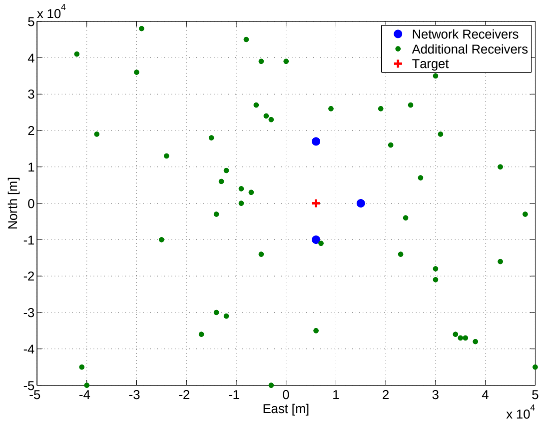

Fig. 9. Augmented configuration: displacement of target and receivers. One receiver is randomly positioned at each step, maintaining the position of the previously added receivers. The positions are plotted in the ENU local frame.

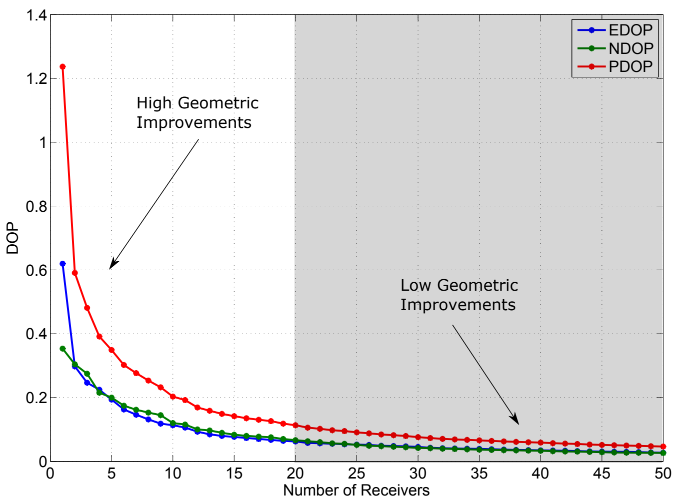

Fig. 10. Values of the EDOP, NDOP and PDOP as a function of the number of additional receivers considered. 20 additional devices seems to be a reasonable limit for a tangible improvement of the geometry.

9 and Fig. 10 are valid for both *Augmented* and *Augmented Degraded* scenarios.

In order to assess the effects of the introduction of additional sources of measurement in the position domain, the performance of the different configurations is evaluated in terms of RMS and maximum errors for East, North and horizontal components.

In Fig. 11, the RMS error values, as a function of the number of additional devices, are shown. Specifically: in the upper box the values relative to the horizontal errors are plotted; in the central and lower boxes the values related to East and North components are shown respectively. The results obtained in the position domains are consistent with the finding in the geometry domain: once again two regions can be identified. The first region is characterized by a high reduction of the RMS errors, which is halved, passing from more than 800 m to almost 400 m, whereas in the second region, the RMS errors are almost constant, confirming the asymptotical behavior

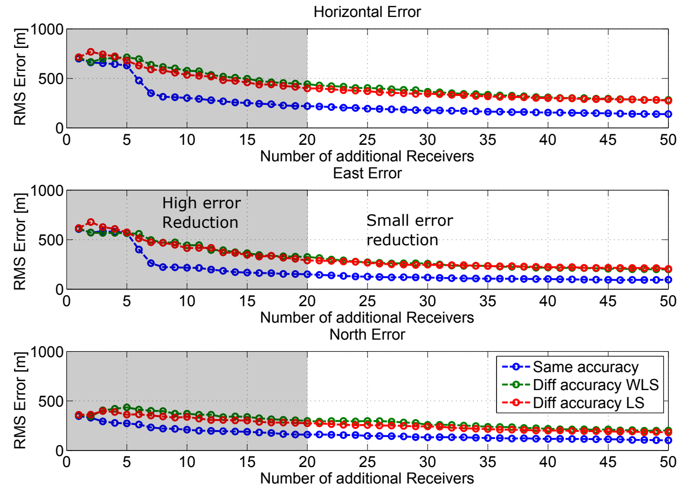

Fig. 11. RMS position errors for the three components as a function of the additional receivers. Three different configurations are considered: receivers with the same accuracy (red line); receivers with degraded accuracy (blue line); receivers with degraded accuracy, weighted accordingly (green line).

shown in the geometry analysis.

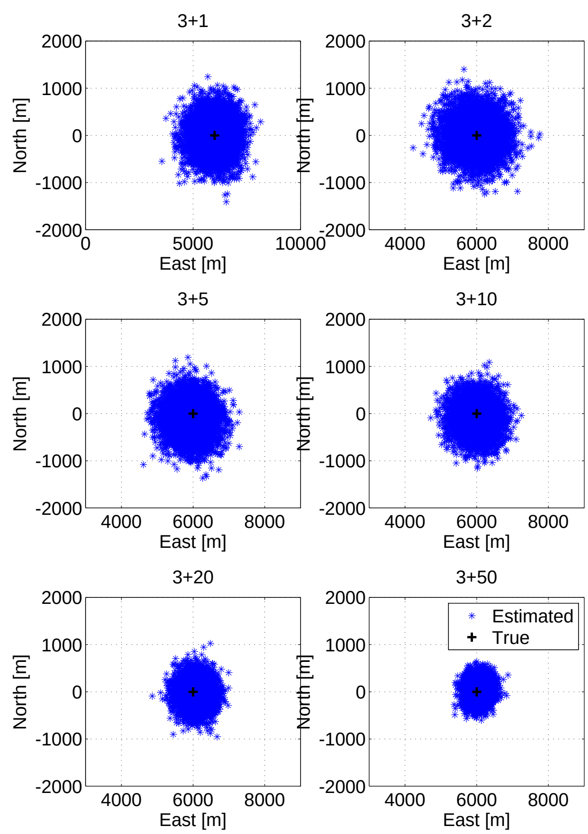

Fig. 12. Horizontal position estimates of the target location. The positions are plotted in the ENU frame. The clouds are centered in the actual target position (black cross).

The analysis of the position domain not only confirms the results in the geometry domain, but allows one to optimize the number of the additional devices as a function of the positioning accuracy required by the application. For example, in case a geofence is employed to limit the access to a restricted area, requiring to estimate the position of the potential intruder with an accuracy of about 500 m, then it is useless to add 50 receivers while 10 are enough to achieve the goal. This *a priori* considerations are useful to limit the displacement-cost of the nodes network and also the overall complexity of the system. Finally, the best performance are obviously obtained using receivers with better accuracy. In case of employment of devices with different accuracies, the Weighted Least Squares (WLS) approach provides a small improvement with respect to the LS. In Fig. 12, the horizontal position estimates of the target location are shown. Once again, the positions are plotted in the ENU frame. In order to avoid the repetition of similar findings, only the results relative to the *Augmented degraded* scenario (worst case) are presented in this picture. From the figures, it can be noted that all the clouds are centered into the actual target position (black cross) and that the size of the clouds is strongly reduced passing from the base-line configuration (upper-left box) to the more complex network (bottom-right box), which exploits 3 base stations and 50 additional receivers. However a relatively small improvement can be noted passing from 20 to 50 additional devices.

IV. Conclusions

This paper investigates and demonstrates the implementation of RF radiolocation with a network of base stations which may include not-synchronized mobile assets with different performance. A *"MN"* algorithm, which allows estimating the different offsets of the included receivers, is introduced and described in detail. The effectiveness of the proposed approach is demonstrated with simulated data in three different scenarios, namely: *'Base-line'*, *'Augmented'* and *'Augmented degraded'*.

The hypotheses to exploit a network of identical, fixed-position base stations for radiolocation purposes at sea is seldom verified in real operative scenarios. More often, in order to rely on a sufficient number of geographically distributed receivers, one needs to include nodes with different characteristics, such as those on board of cooperating vessels or carried by buoys, balloons and Remotely Piloted Aircrafts (RPAs). The research allows estimating the maximum tolerable offset between the receivers included in a network of base stations, whenever the classical TDOA method is employed. The results show that the proposed algorithm is not affected by the increasing of the offset between the receivers, whereas the classical algorithm is strongly dependent on this parameter. A small offset does not tangibly affect the classical algorithm as long as it is absorbed by the measurements noise. Nevertheless, when the offset becomes higher than the measurements noise, the degradation is evident: with an offset larger than $3.3 \cdot 10^{-5}$ sec, the classical algorithm does not converge anymore.

The introduction of additional receivers enhances the geometry condition of the system. In order to assess the improvement, several tests have been carried out, varying the number of added receivers from one to 50. From the analysis, two areas can be identified: the first region (from 1 to 20 additional receivers), where there is an evident reduction of the geometric parameters; the second region (from 21 to 50 additional receivers), where only a small improvement of the geometry can be appreciated. Hence, even though theoretically an infinite number of additional receivers can improve the geometric conditions, 20 additional devices seems to be a reasonable limit to achieve a relevant improvement.

The performance of the *"MN"* is compared with that of the conventional TDOA algorithm in terms of RMS and maximum positioning errors of the target-transmitter. In particular, from the obtained results it appears a strong reduction of the RMS positioning error as a function of the additional number of receivers: the horizontal RMS passes from two kilometers (in case of the *'Base-line'* configuration) to almost 500 meters (in case of the *'Augmented'* configuration). Moreover, by increasing the number of additional receivers, an asymptotical behavior of the RMS error has been observed: from one to 20 additional receivers the position error is significantly reduced, whereas from 20 to 50 receivers the relative improvement is almost negligible. These results confirm the findings of the geometry analysis and analogous conclusions can be drawn from the results relative to the maximum positioning error. Obviously this value is somehow related to the geometry of the receivers network. In fact, if some geo-morphological or geo-political constraint exists, which prevents to displace the receivers within a certain area, then the minimum number of additional receivers necessary to achieve the required accuracy could sensibly vary.

Finally, the simulation results point out the minimum number of additional base stations required to achieve a given accuracy in the estimation of the target-transmitter position. For example, if a geofence network should be used to monitor the access to a restricted area, and an accuracy of 1000 m is required, it is useless to use 50 additional receivers because 10 receivers are enough. This *a-priori* considerations are useful to limit the displacement cost of the nodes network and the overall complexity of the system. The same consideration about the displacement of the additional receivers applies also to this bound.

Future works on this subject shall include real data from not-synchronized mobile receivers with different accuracy, in order to validate the encouraging preliminary results obtained on simulated data.

References

[1] European Parliament and European Council, "Directive 2002/59/EC establishing a community vessel traffic monitoring and information system." Official Journal of the European Communities, June 2002.

[2] Y. Zhou, "An efficient least-squares trilateration algorithm for mobile robot localization," *Proceeding of IEEE/RSJ International Conference on Intelligent Robots and Systems*, October 2009.

[3] F. Thomas and L. Ros, "Revisiting trilateration for robot localization," *IEEE Transactions on Robotics*, 2005.

[4] B. Fang, "Trilateration and extension to global positioning system navigation," *Journal of Guidance*, 1986.

[5] D. E. Manolakis, "Efficient solution and performance analysis of 3-D position estimation by trilateration," *IEEE Transactions on Aerospace and Electronic Systems*, 1996.

[6] F. Papi, D. Tarchi, M. Vespe, F. Oliveri, F. Borghese, G. Aulicino, and A. Vollero, "Radiolocation and Tracking of Automatic Identification System Signals for Maritime Situational Awareness," *IET Radar Sonar and Navigation*, 2015.

[7] C. Gioia, *GNSS Navigation in Difficult Environments: Hybridization and Reliability*. PhD thesis, University Parthenope of Naples, 2014.

[8] A. Panwar, A. Kumar, and S. A. Kumar, "Least Squares Algorithms for Time of Arrival Based Mobile Source Localization and Time Synchronization in Wireless Sensor Networks," *Proceedings published by International Journal of Computer Applications (IJCA) Interna-*

tional Conference on Computer Communication and Networks CSI-COMNET-2011, 2011.

[9] B. Friedlander, "A passive localization algorithm and its accuracy analysis," *IEEE Journal of Oceanic Engineering*, 1987.

[10] I. Guvenc and C. Chong, "A survey on TOA based wireless localization and NLOS mitigation techniques," *IEEE Communications Surveys & Tutorials*, 2009.

[11] P. F. Sammartino, M. Vespe, F. Oliveri, and D. Tarchi, "A new method to verify vessel positions (AIS message). Pre-operational validation and future perspectives," tech. rep., JRC Joint Research Centre, 2015.

[12] Y. Wang, S. Ma, and C. Chen, "TOA-based passive localization in quasi-synchronous network," *IEEE Communications Letters*, 2014.

[13] R. Kaune, "Accuracy Studies for TDOA and TOA Localization," in *Fusion 2012*, 2012.

[14] W. H. Foy, "Position-location solutions by Taylor-series estimation," *IEEE Transactions on Aerospace and Electronics Systems*, 1976.